

# A photo-thermal interaction in semi-conductor medium with cylindrical cavity by analytical and numerical methods

Ibrahim A. Abbas\*

Department of mathematics, Faculty of Science, Sohag University, Sohag, Egypt

(Received March 3, 2021, Revised April 16, 2021, Accepted April 27, 2021)

**Abstract.** In this work, we compare the analytical solutions with the numerical solutions for photothermal interactions in semiconductor medium containing cylindrical cavity. This paper is devoted to a study of the photothermal interactions in semiconductor medium in the context of the coupled photo-thermal model. The basic equations are formulated in the domain of Laplace transform and the eigenvalue scheme are used to get the analytical solutions. The numerical solution is obtained by using the implicit finite difference method (IFDM). A comparison between the analytical solution and the numerical solutions are obtained. It is found that the implicit finite difference method (IFDM) is applicable, simple and efficient for such problems.

**Keywords:** Laplace transforms; finite difference method; semi-conductor mediums; cylindrical cavity; eigenvalue method

## 1. Introduction

To understand the internal structural properties of elastic materials, particularly in semiconductor media, the electric properties of these materials must be studied in consideration their mechanical-thermal properties. Much effort has been made for generalized theories of thermoelasticity in solving thermoelastic models instead of the classical decoupled and coupled theory of thermoelasticity. For decoupled thermoelasticity, the absence of any term reflecting elasticity in the thermal conduction equation does not appear to be real where due to the mechanical loading of an elastic body, the strain causes a change in the temperature field. Moreover, the thermal conduction equation is of the parabolic type of the results of the propagation of thermal waves at an infinite speed, which also contradicts the real physical phenomena. Introduction of the strain rate term in the decoupled thermal conduction equation. The models of bodies explained the properties of the internal structure of medium when used the secondly law of thermodynamic with the development of semiconductor integrated circuit technology and solid-state sensors technology have been widely used in several fields. Previously, micro-mechanical structures of the thermoelasticity and plasma field are analyzed experimental and theoretical as in Todorovic *et al.* (2003), Song *et al.* (2008). Lotfy *et al.* (2020) studied the electro-magnetic and Thomson effects through the photo-thermal transport process of semiconductor material. Hobiny and Abbas (2019) discussed the photothermoelasticity interaction in a two-dimension semiconducting plane under Green-Naghdi theory. Lotfy *et al.* (2020) discussed the responses

of Thomson and electro-magnetic influences of semiconductor material caused by laser pulses under photothermoelastic excitation. Abbas *et al.* (2020) presented the solutions of photo-thermal interaction in a semiconducting materials with cylindrical hole and variable thermal conductivity. Alzahrani (2020) investigated the effects of variable thermal conductivity in semi-conductor materials. Alzahrani and Abbas (2019) discussed the photothermoelasticity interactions in a two-dimension semiconductors mediums without energy dissipation. Lotfy *et al.* (2019) investigated the influences of variable thermal conductivity in semiconductors mediums with cavity under fractional-order magneto-photothermal models. Das *et al.* (2021) studied the electro-magneto-thermo-elastic analysis for a thin circular semiconductor material. Hobiny and Abbas (2017) presented a study on photo-thermal wave in an unbounded semiconductor material with cylindrical cavities

The FDM is a numerical technique that finds an approximate solution of a given problem. The concept of this method is replacing the derivatives that appear in the differential equation by an algebraic approximation. The unknowns of the approximated algebraic equations are the dependent variables at the grid points. Abd-Alla *et al.* (Abd-Alla, Abo-Dahab *et al.*) studied the effects in a thermoelastic annular cylinder using the finite difference method. Abd-Alla *et al.* (2003) studied the effects of nonhomogeneous in an isotropic cylinder under magnetic field. Mukhopadhyay and Kumar (2009) applied the finite difference technique to study the generalized thermoelasticity problem of annular cylinders with variable material properties. Abd-Alla *et al.* (2007) studied the solutions of the transient coupled thermoelastic of an annular fins by the implicit finite-difference technique. Patra *et al.* (2020) used the finite difference technique to study the computational model on thermoelastic analysis

\*Corresponding author, Professor  
E-mail: [ibrabbas7@science.sohag.edu.eg](mailto:ibrabbas7@science.sohag.edu.eg)

with the magnetic field in a rotating cylinder. Several authors (Palani and Abbas 2009, Marin 2010, El-Naggar *et al.* 2013, Abbas and Alzahrani 2016, Abbas and Kumar 2016, Alzahrani and Abbas 2016, Bhatti *et al.* 2019, Itu *et al.* 2019, Lata and Kaur 2019, Marin *et al.* 2019, Riaz *et al.* 2019, Sarkar *et al.* 2019, Lata and Singh 2020, Vinyas *et al.* 2020, Das *et al.* 2021) used the various thermoelastic theories to get the solutions of several problems.

The present paper is an attempt to get new numerical solutions of photo-thermo-elastic problem using the implicit finite difference method (IFDM). Numerical results for the displacement, the carrier density, the temperature and the radial and hoop stresses distributions are presented graphically. Finally, the accuracy of the finite difference method was validated by the comparing between the numerical and the analytical solutions for all physical fields.

## 2. Mathematical model

The governing equations in an isotropic semiconductor medium in the absence of the body force and the thermal sources are presented as in (Mandelis *et al.* 1997, Song *et al.* 2012, Youssef and El-Bary 2018):

$$\mu u_{i,jj} + (\lambda + \mu)u_{j,ij} - \gamma_n N_{,i} - \gamma_t T_{,i} = \rho \frac{\partial^2 u_i}{\partial t^2} \quad (1)$$

$$D_e N_{,jj} - \frac{N}{\tau} + \frac{k}{\tau} T = \frac{\partial N}{\partial t}, \quad (2)$$

$$(KT_{,j})_j + \frac{E_g}{\tau} N - \gamma_t T_o \frac{\partial u_{j,j}}{\partial t} = \rho c_e \frac{\partial T}{\partial t}. \quad (3)$$

$$\sigma_{ij} = (\lambda u_{k,k} - \gamma_t T - \gamma_n N) \delta_{ij} + \mu (u_{i,j} + u_{j,i}), \quad (4)$$

Let us consider a homogeneous isotropic infinite semiconducting medium containing a cylindrical hole. Its state can be expressed in terms of the space variable  $r$  and the time  $t$  which occupying the region  $a \leq r < \infty$ . The cylindrical coordinates  $(r, \theta, z)$  are taken with  $z$ -axis aligned along the cylinder axis. Due to symmetry involved in the problem, only the radial displacement  $u_r = u(r, t)$  is different from zero. Therefore Eqs. (1)-(4) can be expressed according to the following forms:

$$\rho \frac{\partial^2 u}{\partial t^2} = (\lambda + 2\mu) \left( \frac{\partial^2 u}{\partial r^2} + \frac{1}{r} \frac{\partial u}{\partial r} - \frac{u}{r^2} \right) - \gamma_n \frac{\partial N}{\partial r} - \gamma_t \frac{\partial \Theta}{\partial r}, \quad (5)$$

$$\frac{\partial N}{\partial t} = D_e \left( \frac{\partial^2 N}{\partial r^2} + \frac{1}{r} \frac{\partial N}{\partial r} \right) - \frac{N}{\tau} + \frac{\delta}{\tau} \Theta, \quad (6)$$

$$K \left( \frac{\partial^2 \Theta}{\partial r^2} + \frac{1}{r} \frac{\partial \Theta}{\partial r} \right) = -\frac{E_g}{\tau} N + \rho c_e \frac{\partial \Theta}{\partial t} + \gamma_t T_o \frac{\partial}{\partial t} \left( \frac{\partial u}{\partial r} + \frac{u}{r} \right), \quad (7)$$

$$\sigma_{rr} = (\lambda + 2\mu) \frac{\partial u}{\partial r} + \lambda \frac{u}{r} - \gamma_n N - \gamma_t \Theta, \quad (8)$$

$$\sigma_{\theta\theta} = (\lambda + 2\mu) \frac{u}{r} + \lambda \frac{\partial u}{\partial r} - \gamma_n N - \gamma_t \Theta. \quad (9)$$

## 3. Application

The problem initial conditions are defined as

$$u(r, 0) = 0, \frac{\partial u(r, 0)}{\partial t} = 0, T(r, 0) = 0, \frac{\partial T(r, 0)}{\partial t} = 0, N(r, 0) = 0, \frac{\partial N(r, 0)}{\partial t} = 0, \quad (10)$$

While the problem boundary conditions are given as

$$u(a, t) = 0, \quad (11)$$

$$T(0, t) = T_1 H(t) \quad (12)$$

$$D_e \frac{\partial N(x, t)}{\partial x} \Big|_{x=0} - s_b N(x, t) = 0 \quad (13)$$

Now, for appropriateness, the dimensionless physical fields can be given by

$$N' = \frac{N}{n_o}, (T', T'_1) = \frac{(T, T_1)}{T_o}, (r', u') = \xi c(r, u), (\sigma'_{rr}, \sigma'_{\theta\theta}) = \frac{(\sigma_{rr}, \sigma_{\theta\theta})}{\lambda + 2\mu}, (t', \tau') = \xi c^2(t, \tau), \quad (14)$$

where  $c^2 = \frac{\lambda + 2\mu}{\rho}$  and  $\xi = \frac{\rho c_e}{K}$ .

By using the variables of nondimensional forms (14), the basic relations with the neglecting of the dashes can be written by:

$$\frac{\partial^2 u}{\partial t^2} = \frac{\partial^2 u}{\partial r^2} + \frac{1}{r} \frac{\partial u}{\partial r} - \frac{u}{r^2} - x_1 \frac{\partial N}{\partial r} - x_2 \frac{\partial T}{\partial r}, \quad (15)$$

$$x_3 \frac{\partial N}{\partial t} = \frac{\partial^2 N}{\partial r^2} + \frac{1}{r} \frac{\partial N}{\partial r} - \frac{x_3}{\tau} N + \frac{\beta}{\tau} T, \quad (16)$$

$$\frac{\partial^2 T}{\partial r^2} + \frac{1}{r} \frac{\partial T}{\partial r} - \frac{x_4}{\tau} N = \frac{\partial T}{\partial t} + x_5 \frac{\partial}{\partial t} \left( \frac{\partial u}{\partial r} + \frac{u}{r} \right), \quad (17)$$

$$\sigma_{rr} = \frac{\partial u}{\partial r} + x_6 \frac{u}{r} - x_1 N - x_2 T, \quad (18)$$

$$\sigma_{\theta\theta} = x_6 \frac{\partial u}{\partial r} + \frac{u}{r} - x_1 N - x_2 T, \quad (19)$$

$$T(a, t) = T_1 H(t), \quad (20)$$

$$\frac{\partial N(r, t)}{\partial r} \Big|_{r=a} - x_7 N(a, t) = 0 \quad (21)$$

$$u(a, t) = 0 \quad (22)$$

where  $x_1 = \frac{n_o \gamma_n}{\lambda + 2\mu}$ ,  $x_2 = \frac{T_o \gamma_t}{\lambda + 2\mu}$ ,  $x_3 = \frac{1}{\xi D_e}$ ,  $x_4 = \frac{n_o E_g}{\rho c_e T_o}$ ,  $x_5 = \frac{\gamma_t}{\rho c_e}$ ,  $x_6 = \frac{\lambda}{\lambda + 2\mu}$ ,  $x_7 = \frac{s_b}{\xi c D_e}$ ,  $\beta = \frac{\delta T_o}{n_o \xi D_e}$ .

4. Analytical methods

Applying the Laplace transforms for relations (14)-(18) are defined by the formula (Debnath and Bhatta 2014).

$$\bar{f}(r, p) = L[f(r, t)] = \int_0^\infty f(r, t)e^{-pt} dt, p > 0. \quad (23)$$

Hence, the following system are obtained

$$p^2\bar{u} = \frac{d^2\bar{u}}{dr^2} + \frac{1}{r} \frac{d\bar{u}}{dr} - \frac{\bar{u}}{r^2} - x_1 \frac{d\bar{N}}{dr} - x_2 \frac{d\bar{T}}{dr}, \quad (24)$$

$$px_3\bar{N} = \frac{d^2\bar{N}}{dr^2} + \frac{1}{r} \frac{d\bar{N}}{dr} - x_3 \frac{\bar{N}}{\tau} + \frac{\beta}{\tau} \bar{T}, \quad (25)$$

$$\frac{d^2\bar{T}}{dr^2} + \frac{1}{r} \frac{d\bar{T}}{dr} = -\frac{x_4}{\tau} \bar{N} + p\bar{T} + x_5p \left( \frac{d\bar{u}}{dr} + \frac{\bar{u}}{r} \right), \quad (26)$$

$$\bar{\sigma}_{rr} = \frac{d\bar{u}}{dr} + x_6 \frac{\bar{u}}{r} - x_1\bar{N} - x_2\bar{T}, \quad (27)$$

$$\bar{\sigma}_{\theta\theta} = x_6 \frac{d\bar{u}}{dr} + \frac{\bar{u}}{r} - x_1\bar{N} - x_2\bar{T}, \quad (28)$$

$$\bar{T}(a, p) = \frac{1}{p}, \quad (29)$$

$$\left. \frac{d\bar{N}(r, p)}{dr} \right|_{r=a} = x_7\bar{N}(a, p), \quad (30)$$

$$\bar{u}(a, p) = 0, \quad (31)$$

Differentiating Eqs (25) and (26) with respect to  $r$  and using in combination Eq. (24), it is possible to obtain the following expressions:

$$\frac{d^2\bar{u}}{dr^2} + \frac{1}{r} \frac{d\bar{u}}{dr} - \frac{\bar{u}}{r^2} = p^2\bar{u} + x_1 \frac{d\bar{N}}{dr} + x_2 \frac{d\bar{T}}{dr}, \quad (32)$$

$$\begin{aligned} \frac{d^2}{dr^2} \left( \frac{d\bar{N}}{dr} \right) + \frac{1}{r} \frac{d}{dr} \left( \frac{d\bar{N}}{dr} \right) - \frac{1}{r^2} \left( \frac{d\bar{N}}{dr} \right) \\ = x_3 \left( p + \frac{1}{\tau} \right) \frac{d\bar{N}}{dr} - \frac{\beta}{\tau} \frac{d\bar{T}}{dr}, \end{aligned} \quad (33)$$

$$\begin{aligned} \frac{d^2}{dr^2} \left( \frac{d\bar{T}}{dr} \right) + \frac{1}{r} \frac{d}{dr} \left( \frac{d\bar{T}}{dr} \right) - \frac{1}{r^2} \left( \frac{d\bar{T}}{dr} \right) \\ = p^3x_5\bar{u} + \left( px_5x_1 - \frac{x_4}{\tau} \right) \frac{d\bar{N}}{dr} \\ + p(1 + x_5x_2) \frac{d\bar{T}}{dr}. \end{aligned} \quad (34)$$

Now, it is possible to solve the coupled differential Eqs. (32), (33) and (34) by the eigenvalue approach proposed (Das *et al.* 1997, Alzahrani and Abbas 2020, Hobiny and Abbas 2020). From Eqs. (32)-(34), the vector-matrix can be expressed in the following form

$$LV = BV, \quad (35)$$

where

$$L = \frac{d^2}{dr^2} + \frac{1}{r} \frac{d}{dr} - \frac{1}{r^2}, \quad V = \begin{bmatrix} \bar{u} & \frac{d\bar{N}}{dr} & \frac{d\bar{T}}{dr} \end{bmatrix}^T \text{ and } B = \begin{bmatrix} b_{11} & b_{12} & b_{13} \\ 0 & b_{22} & b_{23} \\ b_{31} & b_{32} & b_{33} \end{bmatrix},$$

with

$$\begin{aligned} b_{11} = p^2, b_{12} = x_1, b_{13} = x_2, b_{22} = x_3 \left( p + \frac{1}{\tau} \right), b_{23} = \\ -\frac{\beta}{\tau}, b_{31} = p^3x_5, \\ b_{32} = px_5x_1 - \frac{x_4}{\tau}, b_{33} = p(1 + x_5x_2). \end{aligned}$$

The matrix  $B$  has its characteristic formulation as

$$\begin{aligned} \zeta^3 - \zeta^2(b_{11} + b_{22} + b_{33}) - \zeta(-b_{11}b_{22} + b_{13}b_{31} + b_{23}b_{32} \\ - b_{11}b_{33} - b_{22}b_{33}) + b_{13}b_{22}b_{31} \\ - b_{12}b_{23}b_{31} + b_{11}b_{23}b_{32} - b_{11}b_{22}b_{33} \\ = 0, \end{aligned} \quad (36)$$

The eigenvalues of matrix  $B$  are the three roots of Eq. (39) which are named here  $\zeta_1, \zeta_2, \zeta_3$ . Thus, the corresponding eigenvector  $X = [X_1, X_2, X_3]$  can be calculated as:

$$X_1 = b_{13}(-\zeta + b_{22}) - b_{12}b_{23}, X_2 = -\zeta b_{23}, X_3 = \frac{(\zeta - b_{11})(\zeta - b_{22})}{(\zeta - b_{11})}. \quad (37)$$

The solution of Eq. (38) which is bounded as  $r \rightarrow \infty$  are expressed by

$$V(r, p) = \sum_{i=1}^3 A_i X_i K_1(m_i r), \quad (38)$$

In Eq. (38)  $m_i = \sqrt{\zeta_i}$ ,  $K_1$  is the modified of Bessel's function of order one,  $A_1, A_2$  and  $A_3$  are constants that can be calculated by using the problem boundary conditions. Hence, the field variables have the solutions with respect to  $r$  and  $p$  in the forms:

$$\bar{u}(r, p) = \sum_{i=1}^3 A_i U_i K_1(m_i r), \quad (39)$$

$$\bar{N}(r, p) = -\sum_{i=1}^3 A_i \frac{N_i}{m_i} K_0(m_i r), \quad (40)$$

$$\bar{T}(r, p) = -\sum_{i=1}^3 A_i \frac{T_i}{m_i} K_0(m_i r), \quad (41)$$

$$\begin{aligned} \bar{\sigma}_{rr}(r, p) = \sum_{i=1}^3 A_i \left( \frac{-m_i^2 U_i + x_1 N_i + x_2 T_i}{m_i} K_0(m_i r) \right. \\ \left. + \frac{(x_6 - 1) U_i}{r} K_1(m_i r) \right), \end{aligned} \quad (42)$$

$$\begin{aligned} \bar{\sigma}_{\theta\theta}(r, p) = \sum_{i=1}^3 A_i \left( \frac{-x_6 m_i^2 U_i + x_1 N_i + x_2 T_i}{m_i} K_0(m_i r) \right. \\ \left. - \frac{(x_6 - 1) U_i}{r} K_1(m_i r) \right), \end{aligned} \quad (43)$$

The numerical inversion method adopted the final solutions of the temperature, the displacement, the carrier density and the stress distributions. The Stehfest approach (Stehfest 1970) can be given by

$$f(x, t) = \frac{\ln(2)}{t} \sum_{n=1}^G V_n \bar{f}\left(x, n \frac{\ln(2)}{t}\right), \tag{44}$$

with

$$V_n = (-1)^{\binom{G+1}{\frac{n}{2}}} \sum_{p=\frac{n+1}{2}}^{\min(n, \frac{G}{2})} \frac{(2p)! p^{\binom{G+1}{2}}}{p!(n-p)! \binom{G-p}{2} (2n-1)!},$$

where  $G$  is the term numbers

### 5. Numerical methods

The basic relations obtained are linear partial differential equations. For the solutions problem, the implicit finite difference method (IFDM) is used. The solutions domain  $0 \leq r \leq R_f$ ,  $0 \leq t \leq t_f$ , are replaced by grids described by the set of nodes points  $(r_m, t_s)$ , in which  $r_m = mh$ ,  $m = 0, 1, 2, \dots, M$  and  $t_s = sk$ ,  $s = 0, 1, 2, \dots, S$ . Therefore,  $k = \frac{t_f}{S}$ ,  $h = \frac{r_f}{M}$  are taken as the time step and mess width respectively. For the time derivatives and the space derivatives, the derivatives are replaced the central differences. Thus, the approximations of finite difference method for the system of partial differential equations with respect to the independent variables:

$$\frac{\partial f}{\partial t} = \frac{f_m^{s+1} - f_m^{s-1}}{2k} + o(k^2), \frac{\partial^2 f}{\partial t^2} = \frac{f_m^{s+1} - 2f_m^s + f_m^{s-1}}{k^2} + o(k^2), \tag{45}$$

$$\frac{\partial f}{\partial r} = \frac{f_{m+1}^{s+1} - f_{m-1}^{s+1}}{2h} + o(h^2), \frac{\partial^2 f}{\partial r^2} = \frac{f_{m+1}^{s+1} - 2f_m^{s+1} + f_{m-1}^{s+1}}{h^2} + o(h^2), \tag{46}$$

Eqs. (15)-(19) are then replaced by the implicit finite difference equations by

$$\frac{u_{m+1}^{s+1} - 2u_m^{s+1} + u_{m-1}^{s+1}}{h^2} + \frac{u_{m+1}^{s+1} - u_{m-1}^{s+1}}{2hr_m} - \frac{u_m^{s+1}}{r_m^2} - x_1 \frac{N_{m+1}^{s+1} - N_{m-1}^{s+1}}{2h} - x_2 \frac{T_{m+1}^{s+1} - T_{m-1}^{s+1}}{2h} - \frac{u_{m+1}^{s+1} - 2u_m^{s+1} + u_{m-1}^{s+1}}{k^2} = 0, \tag{47}$$

$$\frac{N_{m+1}^{s+1} - 2N_m^{s+1} + N_{m-1}^{s+1}}{h^2} + \frac{N_{m+1}^{s+1} - N_{m-1}^{s+1}}{2hr_m} - \frac{x_4}{\tau} N_m^{s+1} + \frac{\beta}{\tau} T_m^{s+1} - x_3 \frac{N_m^{s+1} - N_m^{s-1}}{2k} = 0, \tag{48}$$

$$\frac{T_{m+1}^{s+1} - 2T_m^{s+1} + T_{m-1}^{s+1}}{h^2} + \frac{T_{m+1}^{s+1} - T_{m-1}^{s+1}}{2hr_m} + \frac{x_4}{\tau} N_m^{s+1} - x_5 \frac{u_{m+1}^{s+1} - u_{m-1}^{s+1} + u_{m+1}^{s-1} - u_{m-1}^{s-1}}{4hk} - x_5 \frac{u_m^{s+1} - u_m^{s-1}}{2kr_m} - \frac{T_{m+1}^{s+1} - T_{m-1}^{s-1}}{2k} = 0, \tag{49}$$

$$\sigma_{rr} = \frac{u_{m+1}^s - u_{m-1}^s}{2h} + x_6 \frac{u_m^s}{r_m} - x_1 N_m^s - x_2 T_m^s, \tag{50}$$

$$\sigma_{\theta\theta} = x_6 \frac{u_{m+1}^s - u_{m-1}^s}{2h} + \frac{u_m^s}{r_m} - x_1 N_m^s - x_2 T_m^s. \tag{51}$$

### 6. Results and discussion

To illustrate the problem and comparing the theoretical results in the context of coupled photothermal theory, we will present some numerical results and plot several graphs. The values of constants for silicon (Si) material are given by (Song *et al.* 2014):

$$T_o=300(k), d_n=9 \times [10]^{-31} (m^3), \mu=5.46 \times [10]^{10} (N)(m^{-2}), \lambda=3.64 \times [10]^{10} (N)(m^{-2}), E_g=1.11 (eV), \alpha_t=3 \times [10]^{-6} (k^{-1}), c_e=695(J)(kg)^{-1} (k^{-1}), \rho=2330(kg)(m^{-3}), D_e=2.5 \times [10]^{-3} (m^2)(s^{-1}), s_b=2 (m)(s^{-1}), n_o=[10]^{20} (m^{-3}), T_1=1, \tau=[5 \times 10]^{-5} (s).$$

The numerical techniques, outlined above, were used for the distributions of the temperature, the radial displacement, the carrier density, the radial and hoop stress distributions with respect to the r-direction in the context of coupled photothermal model. The calculations were carried out for different values of time and all the variables are taken in the dimensional forms and their graphical are presented in Figs. 1-5. Based on the above data, the physical quantities variations via the radial distance r under the coupled model of thermo-elastic and plasma waves are represented in Figs. 1-5. Fig. 2 displays the temperature variation via the radial distance r. It is observed that the temperature equivalent to the constant temperature the constant temperature  $T_1$  value which satisfy the problem boundary condition on the surface of cavity  $r=1$  then the temperature decreases with the increasing of the radial distance r till it closes to zeros. Fig. 2 shows the carrier density variations via the radial distances r. It is observed that the carrier density starts with its maximum value on the surface of cavity  $r=1$  then the carrier density decreases gradually with the increasing of the radial distance r till it reach to zero value. Fig. 3 shows the displacement variation via the radial distance r. It is observed that the displacement begins from the zeros values which satisfy the problem boundary conditions of on the inner surface of cavity  $r=1$  after that it progressively increases up to peak values then decreases progressively with the increasing of the radial distance r till it reach to

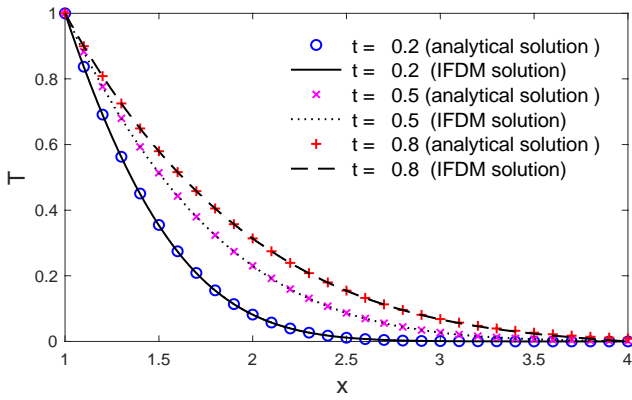


Fig. 1 The temperature variation via the distance

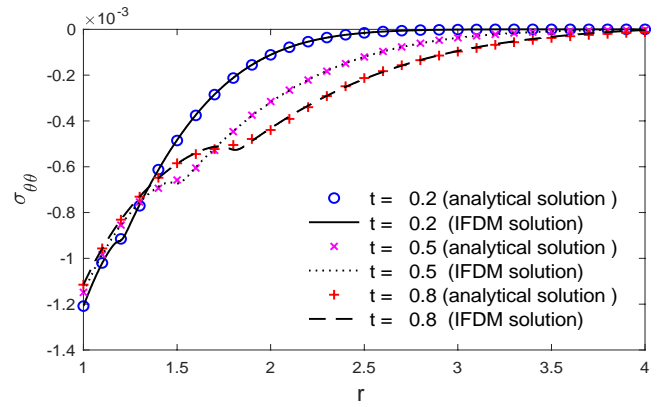


Fig. 5 The hoop stress variations via the distance

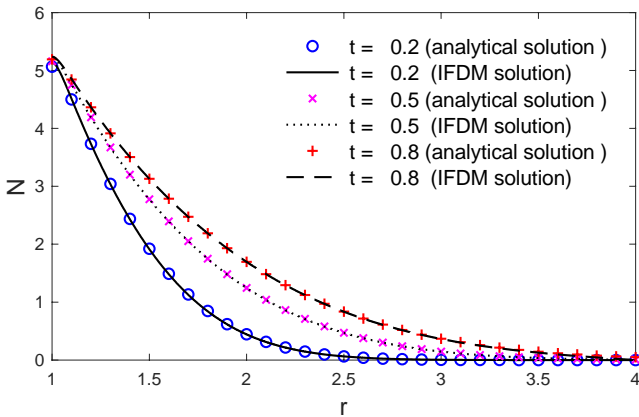


Fig. 2 The carrier density variation via the distance

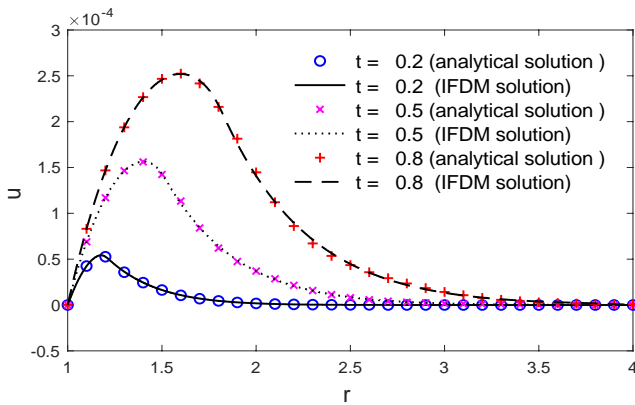


Fig. 3 The displacement variations via the distance

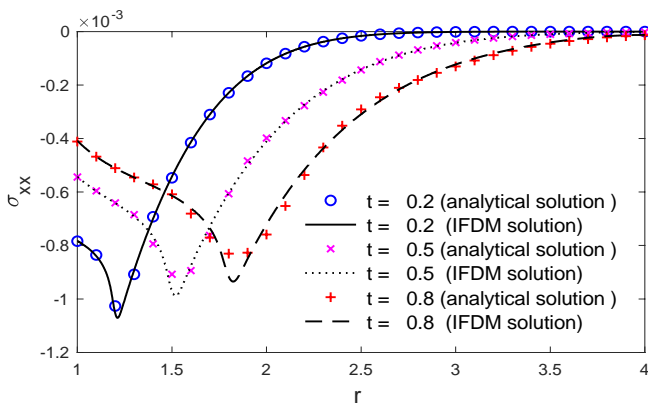


Fig. 4 The radial stress variations via the distance

zeros values. Fig. 4 depicts the radial stress variation via the radial distance  $r$ . It is observed that it attains some negative values then the magnitudes of stress gradually increase up to peak negative values after that the stress gradually increases to zeros values. Fig. 5 depicts the hoop stress variations via the radial distance  $r$ . It is noticed that the hoop stress attains some negative values then the magnitudes of stress decrease gradually to zeros values. The compressions between the solutions, one can conclude that considering the coupled photo-thermal model have major effects on the physical quantities distributions. Figs. 1-5 illustrate the solutions obtained numerically by the implicit finite difference method (IFDM) overlaid onto the solutions obtained analytically. The accuracy of the implicit finite difference method (IFDM) formulation was validated by comparing the analytical and numerical solutions for the field quantities.

### 7. Conclusions

In this work, the coupled of plasma and thermo-elastic waves in a semi-conductor medium with cylindrical cavity is studied. Analytical expressions for the temperature, the carrier density, the displacement and the radial and hoop stresses in the material have been obtained. Also, the numerical solutions were obtained by the implicit finite difference method (IFDM). The accuracy of the implicit finite difference method (IFDM) formulation was validated by comparing the analytical and numerical solutions for the field quantities.

### Acknowledgments

This work was funded by the Academy of Scientific Research and Technology, Egypt, under Science UP grant No. (6473). The authors, therefore, acknowledge with thanks the Academy of Scientific Research and Technology for financial support.

### References

Abbas, I., Hobiny, A. and Marin, M. (2020), "Photo-thermal interactions in a semi-conductor material with cylindrical

- cavities and variable thermal conductivity”, *J. Taibah Univ. Sci.*, **14**(1), 1369-1376.  
<https://doi.org/10.1080/16583655.2020.1824465>.
- Abbas, I.A. and Alzahrani, F.S. (2016), “Analytical solution of a two-dimensional thermoelastic problem subjected to laser pulse”, *Steel Compos. Struct.*, **21**(4), 791-803.  
<https://doi.org/10.12989/scs.2016.21.4.791>.
- Abbas, I.A. and Kumar, R. (2016), “2D deformation in initially stressed thermoelastic half-space with voids”, *Steel Compos. Struct.*, **20**(5), 1103-1117.  
<http://doi.org/10.12989/scs.2016.20.5.1103>.
- Abd-Alla, A., El-Naggar, A. and Fahmy, M. (2003), “Magneto-thermoelastic problem in non-homogeneous isotropic cylinder”, *Heat Mass Transfer*, **39**(7), 625-629.  
<https://doi.org/10.1007/s00231-002-0370-3>.
- Abd-Alla, A., Salama, A., Abd-Ei-Salam, M. and Hosham, H. (2007), “An implicit finite-difference method for solving the transient coupled thermoelasticity of an annular fin”, *Appl. Math. Inf. Sci.*, **1**(1), 79-93.
- Abd-Alla, A.M., Abo-Dahab, S.M. and Kilany, A.A. (2021), “Finite difference technique to solve a problem of generalized thermoelasticity on an annular cylinder under the effect of rotation”, *Numer. Meth. Partial Differential Eq.*, **37**(3), 2634-2646. <https://doi.org/10.1002/num.22753>.
- Alzahrani, F. (2020), “The effects of variable thermal conductivity in semiconductor materials photogenerated by a focused thermal shock”, *Mathematics*, **8**(8), 1230.  
<https://doi.org/10.3390/math8081230>.
- Alzahrani, F.S. and Abbas, I.A. (2016), “The effect of magnetic field on a thermoelastic fiber-reinforced material under GN-III theory”, *Steel Compos. Struct.*, **22**(2), 369-386.  
<http://doi.org/10.12989/scs.2016.22.2.369>.
- Alzahrani, F.S. and Abbas, I.A. (2019), “Photo-thermo-elastic interactions without energy dissipation in a semiconductor half-space”, *Results Phys.*, **15**, 102805.  
<https://doi.org/10.1016/j.rinp.2019.102805>.
- Alzahrani, F.S. and Abbas, I.A. (2020), “Fractional order GL model on thermoelastic interaction in porous media due to pulse heat flux”, *Geomech. Eng.*, **23**(3), 217-225.  
<http://doi.org/10.12989/gae.2020.23.3.217>.
- Bhatti, M., Ellahi, R., Zeeshan, A., Marin, M. and Ijaz, N. (2019), “Numerical study of heat transfer and Hall current impact on peristaltic propulsion of particle-fluid suspension with compliant wall properties”, *Modern Phys. Lett. B*, **33**(35), 1950439. <https://doi.org/10.1142/S0217984919504396>.
- Das, B., Ghosh, D. and Lahiri, A. (2021), “Electromagnetothermoelastic analysis for a thin circular semiconducting medium”, *J. Therm. Stress.*, **44**(4), 395-408.  
<https://doi.org/10.1080/01495739.2021.1881001>.
- Das, N.C., Lahiri, A. and Giri, R.R. (1997), “Eigenvalue approach to generalized thermoelasticity”, *Indian J. Pure Appl. Math.*, **28**(12), 1573-1594. <https://doi.org/10.1515/ijame-2017-0053>.
- El-Naggar, A., Kishka, Z., Abd-Alla, A., Abbas, I., Abo-Dahab, S. and Elsaqheer, M. (2013), “On the initial stress, magnetic field, voids and rotation effects on plane waves in generalized thermoelasticity”, *J. Comput. Theor. Nanosci.*, **10**(6), 1408-1417. <https://doi.org/10.1166/jctn.2013.2862>.
- Hobiny, A. and Abbas, I. (2019), “A GN model on photothermal interactions in a two-dimensions semiconductor half space”, *Results Phys.*, **15**, 102588.  
<https://doi.org/10.1016/j.rinp.2019.102588>.
- Hobiny, A.D. and Abbas, I.A. (2017), “A study on photothermal waves in an unbounded semiconductor medium with cylindrical cavity”, *Mech. Time-Dependent Mater.*, **21**(1), 61-72.  
<https://doi.org/10.1007/s11043-016-9318-8>.
- Hobiny, A.D. and Abbas, I.A. (2020), “Fractional order thermoelastic wave assessment in a two-dimension medium with voids”, *Geomech. Eng.*, **21**(1), 85-93.  
<http://doi.org/10.12989/gae.2020.21.1.085>.
- Itu, C., Öchsner, A., Vlase, S. and Marin, M.I. (2019), “Improved rigidity of composite circular plates through radial ribs”, *Proc. Inst. Mech. Eng. Part L J. Mater. Des. Appl.*, **233**(8), 1585-1593. <https://doi.org/10.1177/1464420718768049>.
- Lata, P. and Kaur, I. (2019), “Thermomechanical interactions in transversely isotropic thick circular plate with axisymmetric heat supply”, *Struct. Eng. Mech.*, **69**(6), 607-614.  
<http://doi.org/10.12989/sem.2019.69.6.607>.
- Lata, P. and Singh, S. (2020), “Time harmonic interactions in non local thermoelastic solid with two temperatures”, *Struct. Eng. Mech.*, **74**(3), 341-350.  
<http://doi.org/10.12989/sem.2020.74.3.341>.
- Lotfy, K., El-Bary, A., Hassan, W., Alharbi, A. and Almatrafi, M. (2020), “Electromagnetic and Thomson effects during photothermal transport process of a rotator semiconductor medium under hydrostatic initial stress”, *Results Phys.*, **16**, 102983. <https://doi.org/10.1016/j.rinp.2020.102983>.
- Lotfy, K., El-Bary, A. and Tantawi, R. (2019), “Effects of variable thermal conductivity of a small semiconductor cavity through the fractional order heat-magneto-photothermal theory”, *Eur. Phys. J. Plus*, **134**(6), 280.  
<https://doi.org/10.1140/epjp/i2019-12631-1>.
- Lotfy, K., Hassan, W., El-Bary, A. and Kadry, M.A. (2020), “Response of electromagnetic and Thomson effect of semiconductor medium due to laser pulses and thermal memories during photothermal excitation”, *Results Phys.*, **16**, 102877. <https://doi.org/10.1016/j.rinp.2019.102877>.
- Mandelis, A., Nestoros, M. and Christofides, C. (1997), “Thermoelectronic-wave coupling in laser photothermal theory of semiconductors at elevated temperatures”, *Opt. Eng.*, **36**(2), 459-468. <https://doi.org/10.1117/1.601217>.
- Marin, M. (2010), “Lagrange identity method for microstretch thermoelastic materials”, *J. Math. Anal. Appl.*, **363**(1), 275-286.  
<https://doi.org/10.1016/j.jmaa.2009.08.045>.
- Marin, M., Vlase, S., Ellahi, R. and Bhatti, M.M. (2019), “On the partition of energies for the backward in time problem of thermoelastic materials with a dipolar structure”, *Symmetry*, **11**(7), 863. <https://doi.org/10.3390/sym11070863>.
- Mukhopadhyay, S. and Kumar, R. (2009), “Solution of a problem of generalized thermoelasticity of an annular cylinder with variable material properties by finite difference method”, *Comput. Meth. Sci. Technol.*, **15**(2), 169-176.  
<https://doi.org/10.12921/cmst.2009.15.02.169-176>.
- Palani, G. and Abbas, I. (2009), “Free convection MHD flow with thermal radiation from an impulsively-started vertical plate”, *Nonlin. Anal. Modell. Control*, **14**(1), 73-84.  
<https://doi.org/10.15388/NA.2009.14.1.14531>.
- Patra, S., Shit, G. and Das, B. (2020), “Computational model on magnetothermoelastic analysis of a rotating cylinder using finite difference method”, *Waves Random Complex Media*, 1-18.  
<https://doi.org/10.1080/17455030.2020.1831710>.
- Riaz, A., Ellahi, R., Bhatti, M.M. and Marin, M. (2019), “Study of heat and mass transfer in the Eyring–Powell model of fluid propagating peristaltically through a rectangular compliant channel”, *Heat Transfer Res.*, **50**(16).  
<https://doi.org/10.1615/HeatTransRes.2019025622>.
- Sarkar, N., Ghosh, D. and Lahiri, A. (2019), “A two-dimensional magneto-thermoelastic problem based on a new two-temperature generalized thermoelasticity model with memory-dependent derivative”, *Mech. Adv. Mater. Struct.*, **26**(11), 957-966. <https://doi.org/10.1080/15376494.2018.1432784>.
- Song, Y., Bai, J. and Ren, Z. (2012), “Study on the reflection of photothermal waves in a semiconducting medium under generalized thermoelastic theory”, *Acta Mech.*, **223**(7), 1545-1557. <https://doi.org/10.1007/s00707-012-0677-1>.

<p>Song, Y., Cretin, B., Todorovic, D.M. and Vairac, P. (2008), “Study of photothermal vibrations of semiconductor cantilevers near the resonant frequency”, <i>J. Phys. D Appl. Phys.</i>, <b>41</b>(15), 155106. <a href="https://doi.org/10.1088/0022-3727/41/15/155106">https://doi.org/10.1088/0022-3727/41/15/155106</a>.</p> <p>Song, Y., Todorovic, D.M., Cretin, B., Vairac, P., Xu, J. and Bai, J. (2014), “Bending of semiconducting cantilevers under photothermal excitation”, <i>Int. J. Thermophys.</i>, <b>35</b>(2), 305-319. <a href="https://doi.org/10.1007/s10765-014-1572-x">https://doi.org/10.1007/s10765-014-1572-x</a>.</p> <p>Stehfest, H. (1970), “Algorithm 368: Numerical inversion of Laplace transforms [D5]”, <i>Commun. ACM.</i> <b>13</b>(1), 47-49. <a href="https://doi.org/10.1145/361953.361969">https://doi.org/10.1145/361953.361969</a>.</p> <p>Todorović, D. (2003), “Photothermal and electronic elastic effects in microelectromechanical structures”, <i>Rev. Sci. Instrument.</i>, <b>74</b>(1), 578-581. <a href="https://doi.org/10.1063/1.1520324">https://doi.org/10.1063/1.1520324</a>.</p> <p>Todorović, D. (2003), “Plasma, thermal, and elastic waves in semiconductors”, <i>Rev. Sci. Instrument.</i>, <b>74</b>(1), 582-585. <a href="https://doi.org/10.1063/1.1523133">https://doi.org/10.1063/1.1523133</a>.</p> <p>Vinyas, M., Harursampath, D. and Kattimani, S. (2020), “Thermal response analysis of multi-layered magneto-electro-thermo-elastic plates using higher order shear deformation theory”, <i>Struct. Eng. Mech.</i>, <b>73</b>(6), 667-684. <a href="http://doi.org/10.12989/sem.2020.73.6.667">http://doi.org/10.12989/sem.2020.73.6.667</a>.</p> <p>Youssef, H.M. and El-Bary, A.A. (2018), “Theory of hyperbolic two-temperature generalized thermoelasticity”, <i>Mater. Phys. Mech.</i>, <b>40</b> 158-171. <a href="http://doi.org/10.18720/MPM.4022018_4">http://doi.org/10.18720/MPM.4022018_4</a>.</p>	<p><math>s_b</math> the speed of recombination on the surface</p> <p><math>u_i</math> the displacement components</p> <p><math>\rho</math> the density of material</p> <p><math>T_1</math> the constant temperature</p> <p><math>H(t)</math> the Heaviside unit function</p>
--	--

GC

**Nomenclature**

- $N = n - n_o, n_o$  the carrier concentration at equilibrium,
- $\gamma_n = (3\lambda + 2\mu)d_n, d_n$  the electronic deformation coefficient,
- $\delta = \frac{\partial n_o}{\partial T}$  the coupling parameter of thermal activation
- $K$  the thermal conductivity
- $\gamma_t = (3\lambda + 2\mu)\alpha_t, \alpha_t$  the linear thermal expansion coefficients
- $c_e$  the specific heat at constant strain
- $\tau$  the lifetime of photo-generated carrier
- $\sigma_{ij}$  the components of stresses
- $D_e$  the carrier diffusion coefficient
- $\lambda, \mu$  the Lamé's constants
- $T = T^* - T_o, T^*$  the variations of temperature
- $T_o$  the reference temperature
- $t$  The time
- $t_f$  the final value of time
- $x_f$  the final value of length